

THROMBOSIS AND HEMOSTASIS

A systems approach to hemostasis: 3. Thrombus consolidation regulates intrathrombus solute transport and local thrombin activity

Timothy J. Stalker,¹ John D. Welsh,^{1,2} Maurizio Tomaiuolo,¹ Jie Wu,¹ Thomas V. Colace,¹ Scott L. Diamond,² and Lawrence F. Brass¹

¹Department of Medicine and ²Department of Chemical and Biomolecular Engineering, University of Pennsylvania, Philadelphia, PA

Key Points

- β_3 integrin tyrosine phosphorylation regulates thrombus consolidation in vivo.
- Intrathrombus solute transport regulates local thrombin activity and platelet activation during hemostatic thrombus formation in vivo.

Hemostatic thrombi formed after a penetrating injury have a distinctive structure in which a core of highly activated, closely packed platelets is covered by a shell of less-activated, loosely packed platelets. We have shown that differences in intrathrombus molecular transport emerge in parallel with regional differences in platelet packing density and predicted that these differences affect thrombus growth and stability. Here we test that prediction in a mouse vascular injury model. The studies use a novel method for measuring thrombus contraction in vivo and a previously characterized mouse line with a defect in integrin $\alpha_{IIb}\beta_3$ outside-in signaling that affects clot retraction ex vivo. The results show that the mutant mice have a defect in thrombus consolidation following vascular injury, resulting in an increase in intrathrombus transport rates and, as predicted by computational modeling, a decrease in thrombin activity and platelet activation in the thrombus core. Collectively, these data (1) demonstrate that in addition to the activation state of individual platelets, the physical properties of the accumulated mass of adherent platelets is critical in determining intrathrombus agonist distribution and platelet activation and (2) define a novel role for integrin signaling in the regulation of intrathrombus transport rates and localization of thrombin activity. (*Blood*. 2014;124(11):1824-1831)

Introduction

In previous studies, we and others have shown that the extent of platelet activation during the hemostatic response to penetrating injuries is heterogeneous, resulting in a distinctive thrombus architecture that consists of a core of fully activated platelets immediately adjacent to the site of injury overlaid by a shell of minimally activated platelets.¹⁻⁶ We have also shown that different signaling pathways within the platelet signaling network predominate in different regions of the thrombus, with adenosine 5'-diphosphate/P2Y₁₂ signaling being critical for platelet recruitment and retention in the shell, whereas thrombin signaling drives full platelet activation and firm adhesion in the core.⁵ These findings show how partially overlapping gradients of soluble agonists emanating from the site of injury can support platelet accumulation, promote platelet activation, and produce the characteristic thrombus architecture.

Regional differences within hemostatic thrombi are not limited to the extent of platelet activation. There are physical differences as well. Most notably, our previous studies showed that the core region has reduced porosity and decreased plasma molecule penetration compared with the shell, indicative of increased platelet packing density in the core.⁵ Solute transport in the gaps between platelets is also slower in the core than in the shell, both of which are orders of magnitude slower than in the remaining vessel lumen.⁷ The drop in transport rates occurs soon after platelet accumulation begins, preceding full platelet activation as detected by the appearance of P-selectin on the platelet surface. A computational analysis based on these

observations indicates that diffusion, rather than convection, governs the movement of plasma and platelet-derived molecules in the small gaps between platelets found in the core, and suggests that the observed difference in transport rates is sufficient to confine the accumulation of thrombin to the core.⁸

Based on these findings, we now propose an extended model for hemostasis in which (1) greater platelet packing density in the thrombus core helps to determine local thrombin activity by providing a microenvironment in which thrombin can accumulate and (2) active regulation of platelet packing density contributes to thrombus growth and stability by helping to determine where thrombin is generated and fibrin accumulates. Here we have tested this model by perturbing platelet packing density and measuring its effects on intrathrombus solute transport, localization of thrombin activity, and platelet activation. Doing so required the development of a novel method to measure thrombus consolidation in real time in vivo in mice with a defect in clot retraction. Prior studies have demonstrated that following initial platelet accumulation at a site of vascular injury, the platelet mass rapidly consolidates via platelet-mediated retractile processes.^{9,10} Law et al showed that substituting Phe for Tyr747 and Tyr759 (diYF) in the cytoplasmic domain of the β subunit of $\alpha_{IIb}\beta_3$ inhibits outside-in signaling through the integrin and impairs clot retraction without affecting integrin activation and fibrinogen binding.¹¹ Here, we have tested the same diYF mice following vascular injury using a newly established method for assessing

Submitted January 25, 2014; accepted June 10, 2014. Prepublished online as *Blood* First Edition paper, June 20, 2014; DOI 10.1182/blood-2014-01-550319.

The online version of this article contains a data supplement.

There is an Inside *Blood* Commentary on this article in this issue.

The publication costs of this article were defrayed in part by page charge payment. Therefore, and solely to indicate this fact, this article is hereby marked "advertisement" in accordance with 18 USC section 1734.

© 2014 by The American Society of Hematology

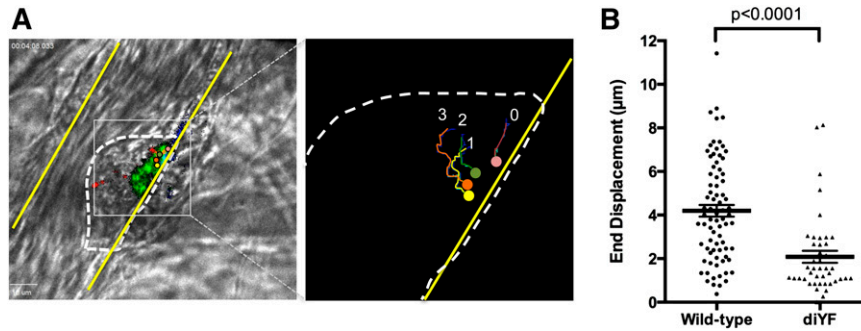


Figure 1. Loss of $\beta 3$ integrin tyrosine phosphorylation attenuates platelet mass consolidation following vascular injury in vivo. Platelet mass consolidation was monitored by tracking the movement of individual platelets following adhesion to a developing thrombus, as described in Methods. (A) Photomicrographs show representative thrombus from a WT mouse. The panel on the left shows 4 fluorescently labeled platelets within the platelet mass (outlined by the dotted line). The panel on the right shows the region in the left panel outlined by the gray box. The movement of the 4 platelets was tracked over time using image analysis software, and the tracks of each platelet in the image can be seen. (B) The movement of individual WT and diYF platelets during laser-induced thrombus formation is reported as the end displacement (total distance along a straight line from platelet starting point to endpoint). Horizontal line and error bars indicate the mean \pm SEM. For WT, $n = 78$ platelets from 14 thrombi and for diYF $n = 43$ platelets from 12 thrombi. Statistics were calculated using the Mann-Whitney test.

molecular transport in the gaps between platelets.⁷ The results show that the diYF mice have a defect in thrombus mass consolidation and that this defect is accompanied by the increase in transport rates and a decrease in fibrin accumulation in the thrombus core predicted by the computational modeling. Taken together, these studies reveal a novel role for outside-in signaling in the regulation of platelet mass consolidation and intrathrombus solute transport in the gaps between platelets. They also show that physical properties such as platelet packing and molecular transport are integral components of the hemostatic response, helping to determine agonist distribution and platelet activation within an evolving platelet mass.

Methods and materials

Mice

DiYF mice were described previously.^{11,12} They were originally generated in the laboratory of Dr David Phillips at Portola Pharmaceuticals (San Francisco, CA) and were obtained by us from Dr Tatiana Byzova at the Cleveland Clinic Foundation (Cleveland, OH). They are backcrossed on to the C57Bl/6 background at least 7 times,¹² and were therefore compared with C57Bl/6 mice from The Jackson Laboratory as controls. Male mice 8 to 12 weeks of age were used for intravital microscopy experiments. The University of Pennsylvania Institutional Animal Care and Use Committee approved all animal procedures.

Laser-induced injury in mouse cremaster arterioles

The laser-induced thrombosis model as performed here was described in detail previously.⁵ Additional information is provided in the supplemental Methods (see supplemental Data available on the *Blood* Web site).

Platelet mass consolidation was measured using an approach modified from Ono et al.⁹ Blood was drawn from a donor mouse via cardiac puncture using heparin as the anticoagulant and diluted 1:1 with modified Tyrode buffer (4 mM *N*-2-hydroxyethylpiperazine-*N'*-2-ethanesulfonic acid, pH 7.4, 135 mM NaCl, 2.7 mM KCl, 3.3 mM NaH_2PO_4 , 2.4 mM MgCl_2 , 0.1% glucose, and 0.1% bovine serum albumin). Platelet-rich plasma was obtained by centrifugation at 150g for 7 minutes. Alexa Fluor 568-labeled anti-CD41 F(ab)₂ was added for 15 minutes, followed by gel filtration of the platelets to remove plasma proteins and unbound labeling antibody. Approximately 50 million gel-filtered platelets in 200 μL of sterile Tyrode buffer were infused into a recipient mouse prepared for intravital microscopy using standard procedures via a jugular vein cannula. The donor platelets were easily distinguished from the recipient's endogenous platelets via their fluorescent label, and they were incorporated into laser-induced thrombi normally. To assess platelet mass consolidation, time-lapse image captures of thrombus

formation were analyzed offline. Stably adherent donor platelets were identified based on their Alexa Fluor 568 label, and the center of each donor platelet was marked manually frame-by-frame using the Manual Tracking procedure in Slidebook image analysis software (Intelligent Imaging Innovations). Once marked, the straight-line distance from where a platelet first firmly adhered to its final position at the conclusion of the time lapse (3 minutes postinjury) was calculated using Slidebook and is reported as the end displacement. Multiple platelets were tracked in each thrombus and multiple thrombi from several mice were studied.

Intrathrombus solute transport was measured using caged fluorescein coupled to albumin (cAlb) as described in detail in Welsh et al.⁷ A detailed description is provided in the supplemental Methods.

Computational simulation of solute transport

A detailed description of computational methods including model design and parameter description is included in an accompanying manuscript.⁸ Additional information is provided in the supplemental Methods.

Flow cytometry

Mouse blood was obtained via the inferior vena cava using heparin as the anticoagulant, diluted 1:1 in modified Tyrode buffer, and centrifuged at 150g for 7 minutes to obtain platelet-rich plasma. Alexa 647 fibrinogen, anti-P-selectin, and Annexin V were added to separate samples, and the platelets were stimulated with either PAR-4 agonist peptide (AYPGKF; Bachem) for fibrinogen binding and P-selectin expression studies or the combination of AYPGKF and convulxin for Annexin V-binding studies. Platelets were incubated for 15 minutes at 37°C, diluted fivefold with phosphate-buffered saline and fluorescence immediately measured using a BD FACSCalibur flow cytometer with subsequent analysis using FlowJo flow cytometry software.

Statistics

For data obtained from intravital microscopy experiments, statistics were calculated using the Mann-Whitney test for nonparametric data using GraphPad Prism 6.0 software.

Results

Role of $\beta 3$ integrin tyrosine phosphorylation in platelet mass consolidation

Mice in which the 2 tyrosines in the $\beta 3$ cytoplasmic domain have been mutated to Phe (diYF) were described previously.¹¹ Platelets

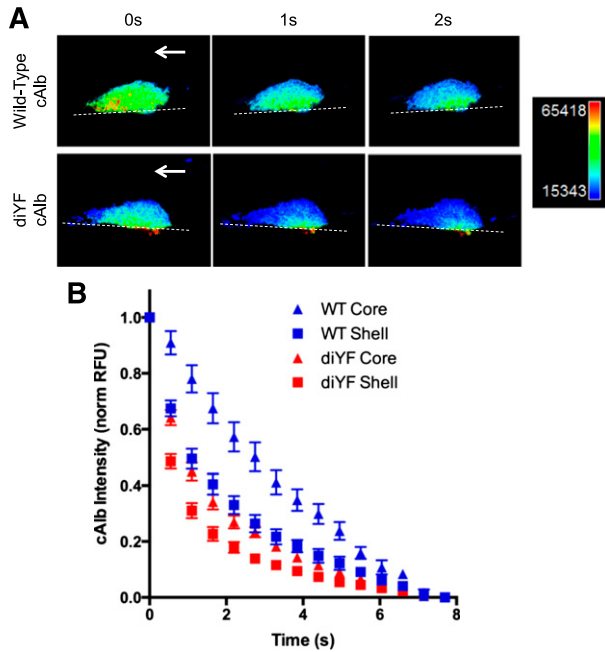


Figure 2. Molecular transport is increased in diYF thrombi. cAlb was used to calculate molecular transport in thrombi formed following laser-induced injury in cremaster arterioles of WT and diYF mice. (A) Photomicrographs show caged-carboxyfluorescein albumin fluorescence within a representative WT and diYF thrombus. The fluorescence is shown in pseudocolor to indicate relative concentration (blue is low, red is high). From left to right, panels show the same WT (top row) or diYF (bottom row) thrombus immediately following a flash of 405-nm laser light to uncage the cAlb in the thrombus (0 seconds), followed by images captured 1 second and 2 seconds after the flash. The decrease in albumin fluorescence from 0 to 2 seconds is due to washout of the albumin from the platelet mass. Note the albumin is retained longer in the core region of the thrombi. (B) Graph shows cAlb washout in the core (P-selectin positive, triangles) and shell (P-selectin negative, squares) regions of WT (blue) and diYF thrombi (red). Quantification and normalization procedure is described in "Methods." Values are mean \pm SEM for $n = 11$ WT and $n = 12$ diYF thrombi.

from diYF mice have normal $\alpha_{IIb}\beta_3$ integrin inside-out activation and ligand binding, but ligand binding–induced β_3 tyrosine phosphorylation is absent.¹¹ Outside-in signaling pathways that require β_3 phosphorylation are thus impaired, resulting in unstable platelet aggregate formation and impaired fibrin clot retraction.¹¹

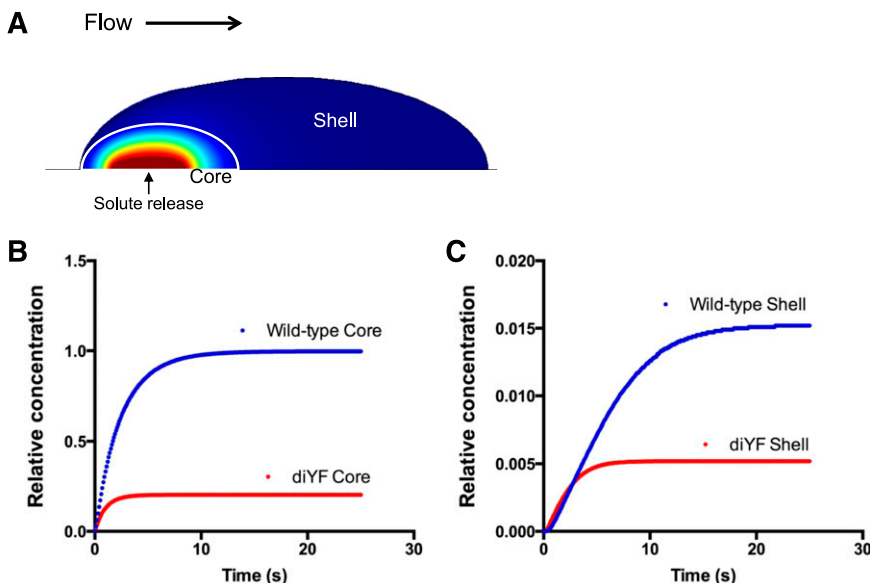


Figure 3. Computational modeling studies demonstrating the impact of impaired platelet mass consolidation on solute distribution within a thrombus. (A) A snapshot of the simulation at steady state showing the core and shell regions, as well as the relative concentration of a solute released at a constant rate from a 3- μ m patch on the vessel wall beneath the core region (shown in pseudocolor: red is high, blue low concentration). (B-C) Graphs depict relative concentration in the core (B) and shell (C) regions of a solute released at a constant rate from the vessel wall beneath the core region. The core and shell regions were defined by values for porosity, permeability, and effective diffusion coefficient that were chosen based on their ability to fit the transport data for WT and diYF mice shown in Figure 2 (as described in Tomaiuolo et al⁸).

Previous reports have used intravital microscopy to observe consolidation of the platelet mass during the early stages of thrombus formation in vivo.^{9,10} Although distinct from fibrin clot retraction in vitro, some of the same signaling mechanisms have been shown to play a role in both processes, including myosin-dependent platelet retraction.^{9,10} Because diYF platelets were previously shown to have a defect in fibrin clot retraction, we sought to determine whether platelet mass consolidation was impaired following vascular injury in diYF mice. To accomplish this goal, we used a single platelet tracking approach in which the movement of individually labeled platelets is tracked as the entire platelet mass consolidates toward the site of injury. In this case, platelets are removed from donor mice, labeled with Alexa 568 anti-CD41 F(ab)₂ fragments, and then infused into a syngeneic recipient mouse in numbers that result in labeling of a small percentage of the circulating platelet pool (described in the Methods section). Penetrating injuries were inflicted in cremaster muscle arterioles using a laser fired through the optics of the microscope.¹³ We have previously shown that the response to laser injury is similar to the response observed when injuries are inflicted with a sharpened glass pipette.⁵

Using this combination of injury and tracking techniques in wild-type mice, individual platelets within the platelet mass may be observed to move toward the site of injury as the mass consolidates with a mean end displacement of $4.2 \pm 0.27 \mu\text{m}$ (mean \pm SEM, Figure 1A-B, supplemental Video 1). The bulk of the consolidation occurred during the first 60 to 90 seconds postinjury. Inward movement was reduced by approximately 50% in thrombi formed in diYF mice, which had a mean end displacement of $2.1 \pm 0.27 \mu\text{m}$ ($P < .0001$ vs wild-type [WT], Figure 1B, supplemental Video 2). These findings demonstrate that platelet mass consolidation is decreased in diYF mouse thrombi.

Intrathrombus solute transport

One possible consequence of impaired platelet mass consolidation in diYF thrombi is altered plasma and solute transport in the narrow spaces between platelets. Intrathrombus solute transport is a critical regulator of platelet activation and thrombus evolution as it determines how far soluble molecular species generated at the injury site (eg, thrombin) may distribute from their source before they are washed out.⁸ Solute transport was measured during hemostatic thrombus

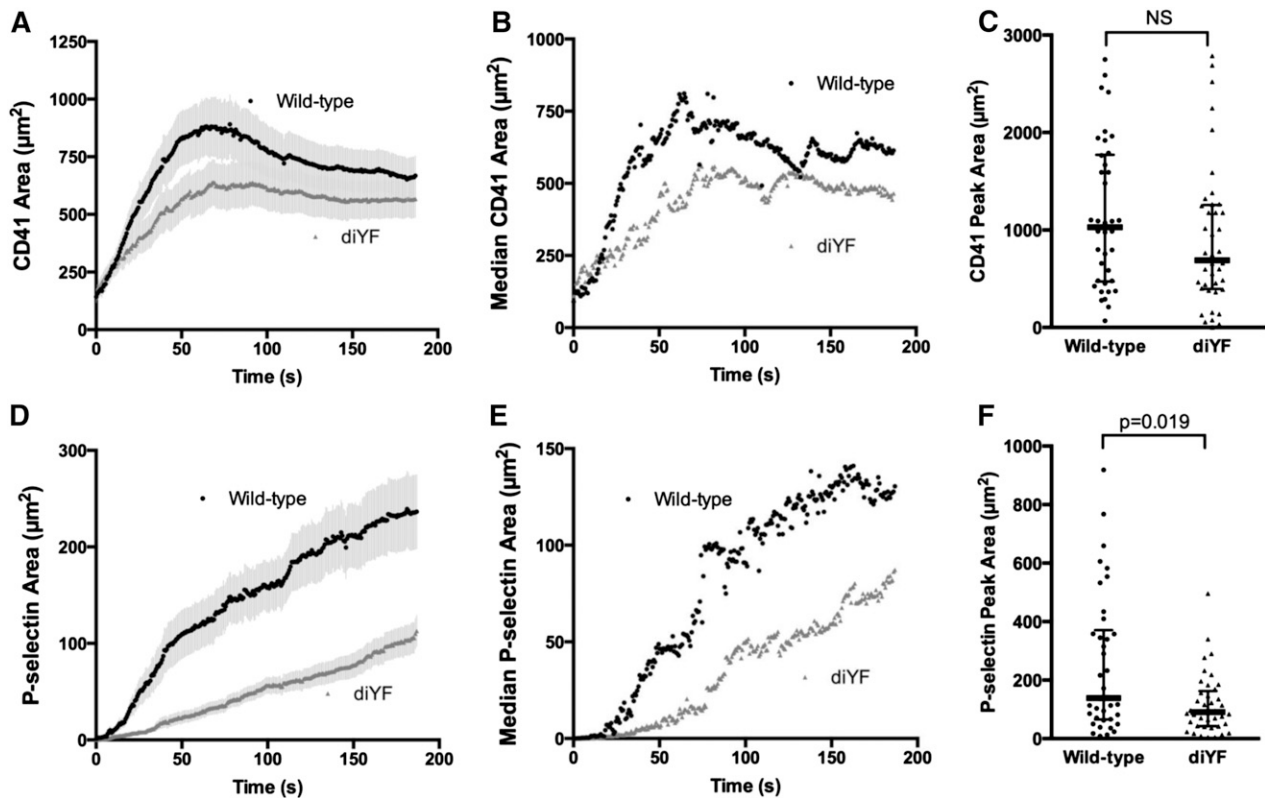


Figure 4. Loss of β_3 integrin tyrosine phosphorylation attenuates platelet activation following vascular injury in vivo. Total platelet accumulation and α -granule secretion were monitored following laser-induced injury in mouse cremaster arterioles using fluorescently tagged antibodies against mouse CD41 and P-selectin, respectively. The graphs in panels A-B and D-E show total platelet accumulation (CD41-positive area; A, mean \pm SEM; B, median) and α -granule secretion (P-selectin-positive area; D, mean \pm SEM; E, median) over time in WT (black circles) and diYF mice (gray triangles). Graphs in panels C and F show peak thrombus (C) and P-selectin-positive (F) areas for WT and diYF mice. The horizontal line and error bars indicate median and interquartile range. For WT, $n = 38$ thrombi from 7 mice and for diYF $n = 41$ thrombi from 6 mice. Statistics were calculated using the Mann-Whitney test for nonparametric data.

formation in vivo using cAlb as described in the Methods section. Following a flash of 405-nm laser light, the washout of the cAlb may be quantified over time to generate decay curves as a measure of solute transport within a platelet mass as a whole or in specific subregions (ie, core and shell regions; Figure 2A-B). Consistent with the findings reported in Welsh et al,⁷ we found that, in WT mice, cAlb washout (ie, solute transport) was substantially slower in the core region of thrombi as compared with the shell region (Figure 2B). This result is consistent with our previously reported finding of decreased porosity (ie, increased platelet density) in the thrombus core vs shell regions.⁵ Interestingly, solute transport was increased relative to controls in both regions of the diYF thrombi, with transport in the core region of diYF thrombi similar to transport in the shell region of WT thrombi (Figure 2B). This finding suggests reduced platelet packing throughout thrombi in diYF mice, consistent with the impaired ability of diYF platelets to retract and consolidate the platelet mass as shown in Figure 1.

Computational simulation of agonist distribution in diYF thrombi

To investigate the impact of altered intrathrombus solute transport on platelet agonist distribution within a thrombus, we used computational modeling to simulate the physical conditions present within WT vs diYF thrombi. Specifically, we examined the impact of the physical microenvironment on the distribution of a protein-sized solute released from the vessel wall at the base of a simulated platelet

mass to mimic thrombin generation at a site of injury in vivo. The Navier-Stokes equations (COMSOL v4.3a) were used to resolve the flow field in a simulated 30- μ m diameter blood vessel with a centerline velocity of 2 mm per second (ie, mimicking a mouse cremaster arteriole). The Brinkman equations¹⁴ were used to solve the velocity field in the thrombus modeled as a porous media and the advection-reaction-diffusion equation was used to simulate the transport of solutes in a porous media describing the hemostatic mass. To simulate the core and shell architecture of WT and diYF thrombi, 2 regions were created in which the porosity, permeability, and effective diffusion coefficient were varied by region to reproduce the solute transport conditions observed in vivo (see Tomaiuolo et al⁸ for details) (Figure 3A). Next, the constant release of a protein-sized solute from a 3 μ m patch below the core region was simulated until a steady state was reached. The concentration of the solute in the core region of diYF thrombi was significantly reduced compared with its concentration in the core of WT thrombi (Figure 3B). The solute concentration was also significantly reduced in the shell of diYF thrombi compared with WT, although it should be noted that very little solute was retained in the shell region in both cases (note the difference in y-axis scale between Figure 3B-C). Thus, these computational simulations suggest that structural differences between the core and shell region can account for the heterogeneity of platelet activation observed in WT mice in vivo, and further predict that altered molecular transport within diYF thrombi will result in reduced local thrombin activity.

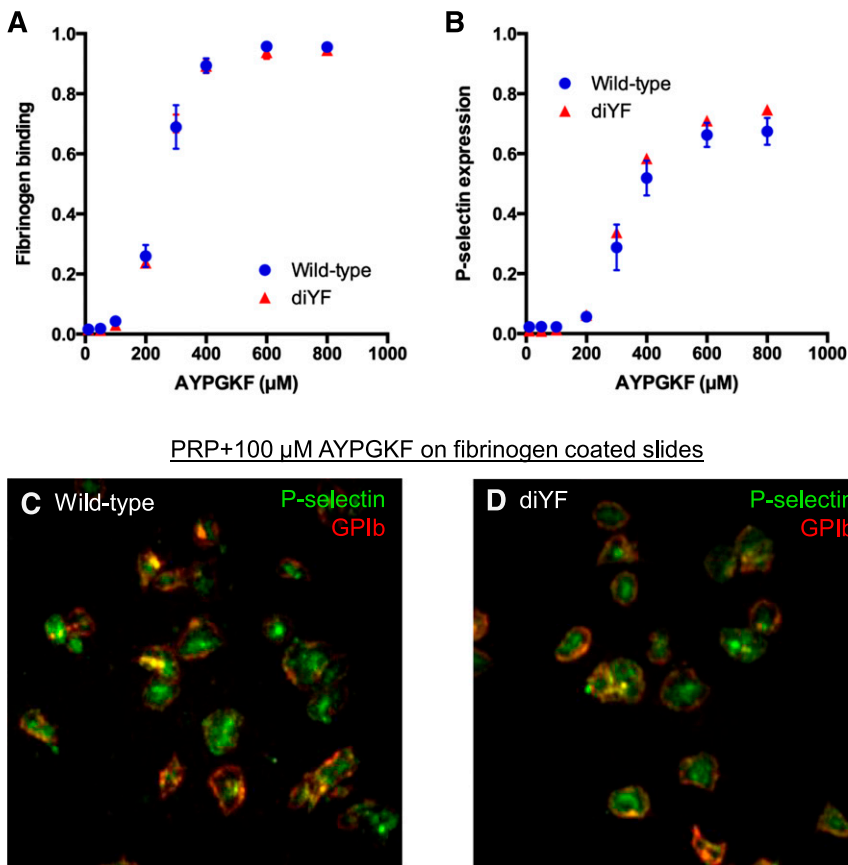


Figure 5. Fibrinogen binding and P-selectin expression are normal in diYF platelets. (A-B) Flow cytometry analysis of fibrinogen binding (A) and P-selectin expression (B) in WT and diYF platelets. Platelets were stimulated with the indicated concentrations of the PAR-4 agonist AYPGKF. Data are expressed as the percentage of positive cells (mean \pm SEM, $n = 3$). (C-D) Representative photomicrographs from WT and diYF platelets showing GPIIb (red) and P-selectin (green) expression by immunofluorescence. Platelets were stimulated with 100- μ M AYPGKF and allowed to spread on immobilized fibrinogen for 45 minutes at 37°C. The cells were fixed and stained with anti-GPIIb and anti-P-selectin without permeabilization to assess surface protein expression.

Laser injury-induced platelet accumulation, activation, and fibrin formation in diYF mice

The above results indicate that $\alpha_{IIb}\beta_3$ outside-in signaling mediated by β_3 integrin tyrosine phosphorylation helps to regulate thrombus architecture and solute transport. Thus, diYF mice serve as a good model to test our hypothesis that thrombus structure and intra-thrombus solute transport are key regulators of agonist distribution and subsequent platelet activation at sites of vascular injury in vivo. We quantified total platelet accumulation, P-selectin expression, and fibrin deposition in diYF mice compared with WT controls following laser-induced injury in mouse cremaster arterioles. Total platelet accumulation was moderately reduced in diYF mice as compared with WT controls (Figure 4A-C), although peak platelet accumulation was not significantly different between the 2 strains (Figure 4C). In both cases, the kinetics of platelet accumulation were comparable to prior reports using this thrombosis model.^{5,13,15} In contrast, the number of P-selectin-positive platelets was significantly reduced in thrombi formed in diYF mice (Figure 4D-F), indicating decreased full platelet activation following vascular injury in vivo in the absence of β_3 integrin tyrosine phosphorylation.

In agreement with prior findings,¹¹ fibrinogen binding by individual diYF platelets in response to the PAR-4 agonist AYPGKF was normal (Figure 5A), demonstrating that the attenuated platelet accumulation and activation in vivo is not related to a direct effect of the diYF mutation on inside-out $\alpha_{IIb}\beta_3$ activation. Furthermore, the ability of diYF platelets to secrete their α -granules and express P-selectin in vitro as assessed by flow cytometry was normal (Figure 5B), as was their ability to mobilize P-selectin to the surface of platelets spread on immobilized fibrinogen (Figure 5C-D). These findings indicate that the defect in P-selectin expression observed in vivo was not due to

reduced P-selectin levels in diYF platelets or a direct effect of β_3 tyrosine phosphorylation-dependent signaling on α -granule secretion.

Fibrin deposition

Prior studies have demonstrated that full platelet activation and α -granule secretion in the laser-induced injury model as used here are primarily due to thrombin-dependent platelet activation.^{2,5,15,16} To determine whether there was reduced thrombin activity in diYF mice, we measured fibrin deposition during thrombus formation. We found that the total area of fibrin deposition was significantly attenuated in diYF mice as compared with WT (Figure 6A-C). Furthermore, the fibrin specifically colocalized with platelets was significantly reduced (Figure 6D-F), suggesting attenuated local thrombin activity within the platelet mass. Importantly, the decrease in fibrin area corresponded to decreased total fibrin accumulation, as quantification of fibrin fluorescence intensity mirrored the results obtained by analyzing fibrin area (supplemental Figure 1A-C). This reduced thrombin activity was not a result of impaired ability of diYF platelets to expose phosphatidylserine on the outer leaflet of the plasma membrane, as Annexin V binding to diYF platelets was normal (supplemental Figure 1D). Thus, it is likely that the reduced thrombin activity observed in diYF mice is attributable to decreased thrombin retention within the platelet mass as a result of impaired platelet packing and increased intrathrombus solute transport.

Discussion

Platelet accumulation at a site of vascular injury is a dynamic process that requires assimilation of chemical and physical cues regarding the

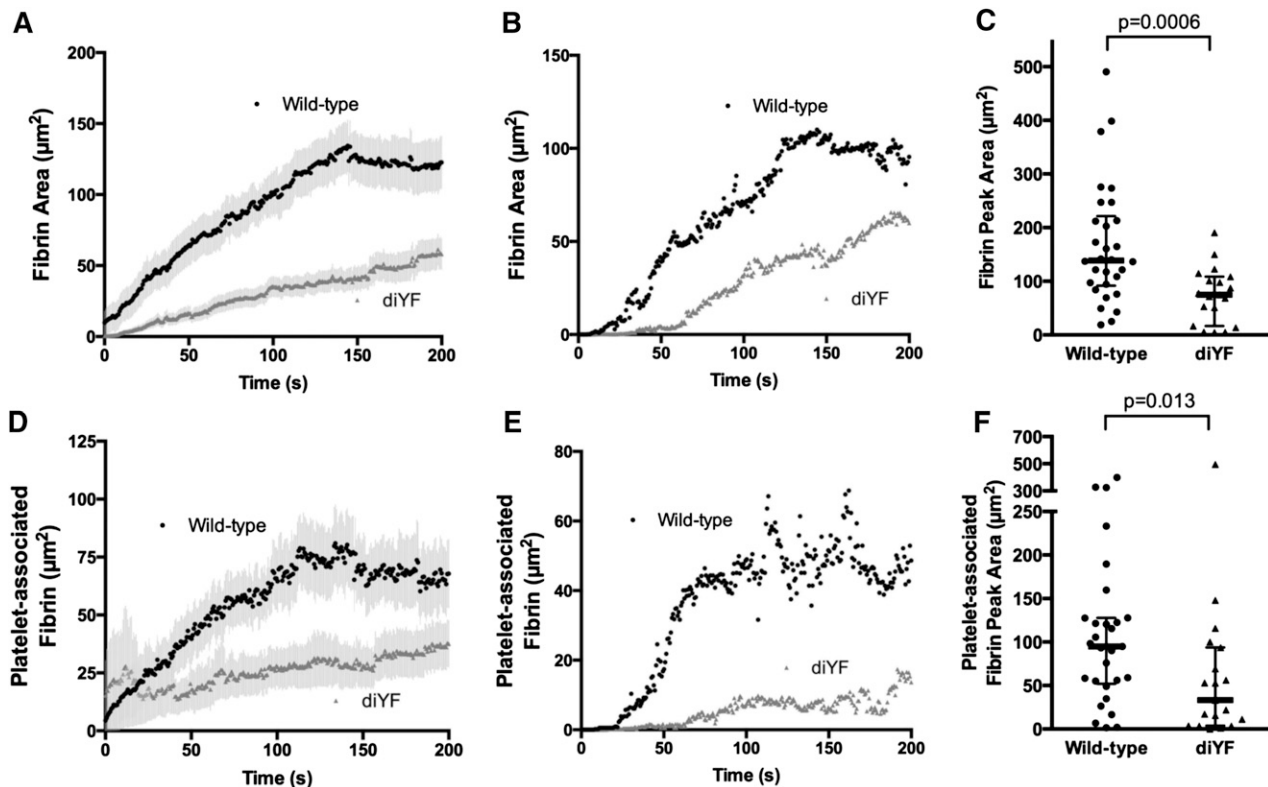


Figure 6. Loss of β_3 integrin tyrosine phosphorylation attenuates fibrin formation following vascular injury in vivo. (A-C) Total fibrin accumulation was monitored following laser-induced injury in mouse cremaster arterioles using a fluorescently tagged antibody that specifically recognizes mouse fibrin. The graphs in panels A and B show total fibrin area (A, mean \pm SEM; B, median) over time. Panel C shows peak fibrin area for WT and diYF mice. The horizontal line and error bars indicate median and interquartile range. (D-F) Platelet-associated fibrin was defined as the area that was positive for both fibrin and CD41 fluorescence. The graphs in panels D and E show platelet-associated fibrin area (D, mean \pm SEM; E, median) over time. Panel F shows peak platelet-associated fibrin area for WT and diYF mice. For WT, $n = 30$ thrombi from 6 mice and for diYF $n = 19$ thrombi from 4 mice. Statistics were calculated using the Mann-Whitney test for nonparametric data.

extracellular environment to promote a cellular response that is coordinated in both time and space to achieve optimal hemostasis. Extensive studies of platelet intracellular signaling pathways over the past several decades have greatly enhanced our understanding of platelet function. Still, it is only by examining platelet function in the complex milieu of an intact vasculature that we can begin to understand how these multiple signaling components are integrated along with contributions from other cells, the vessel wall and local hemodynamic conditions in order to generate a hemostatic plug. In this regard, the current study sought to investigate how a platelet signaling pathway ($\alpha_{IIb}\beta_3$ outside-in signaling), physical characteristics of the platelet mass (platelet mass consolidation), and local molecular transport within the microenvironment of a platelet mass, interact with each other during hemostatic plug formation in vivo. The data demonstrate that each of these components contributes to platelet accumulation and particularly platelet activation following vascular injury. They show that as platelets begin to accumulate at a site of injury they act as physical obstacles, limiting the movement of molecules through the spaces between them. As more platelets accumulate and become activated, outside-in signaling resulting in β_3 phosphorylation contributes to the regulated consolidation of the platelet mass and increased platelet packing density. The increase in packing density results in reduced solute transport within the platelet mass, particularly in the core region. This region of reduced molecular transport provides a protected microenvironment where soluble species such as thrombin generated at the site of injury are retained, leading to robust, irreversible platelet activation (Figure 7). Thus, the platelet response is dictated by the interaction of local

conditions impacting agonist distribution and concentration with the platelet signaling network.

Prior studies have demonstrated that platelet mass consolidation is critical for ensuring the stable accumulation of platelets at a site of injury in vivo.^{9,10} Consolidation is mediated by platelet retraction, as demonstrated by the attenuation of this process by a myosin IIa inhibitor. However, Ono et al found that this process is independent of fibrin formation and therefore distinct from platelet-mediated fibrin clot retraction.⁹ In the present study, we found that mice in which the 2 β_3 cytoplasmic tail NxxY tyrosines are mutated to phenylalanine (diYF) have impaired platelet retraction during platelet accumulation in vivo, resulting in a more loosely packed platelet mass. Thus, β_3 integrin tyrosine phosphorylation is a critical upstream signaling component necessary for efficient platelet mass consolidation in vivo. As primary platelet activation events (including inside-out $\alpha_{IIb}\beta_3$ activation, fibrinogen binding, and granule secretion) are normal when diYF platelets are studied ex vivo, diYF mice provide a unique model in which the role of platelet packing density and platelet mass architecture may be studied independent of direct effects on primary platelet activation pathways.

In conjunction with the impaired platelet mass consolidation seen in diYF mice, we found that intrathrombus transport was increased, allowing molecules to elute out of the platelet mass faster in diYF mice. The importance of solute transport through a thrombus or blood clot has been proposed in several prior studies using combinations of in vitro and theoretical approaches.¹⁷⁻²¹ In general, these studies predicted that the presence of a platelet/fibrin plug will substantially impact solute transport, including movement of coagulation

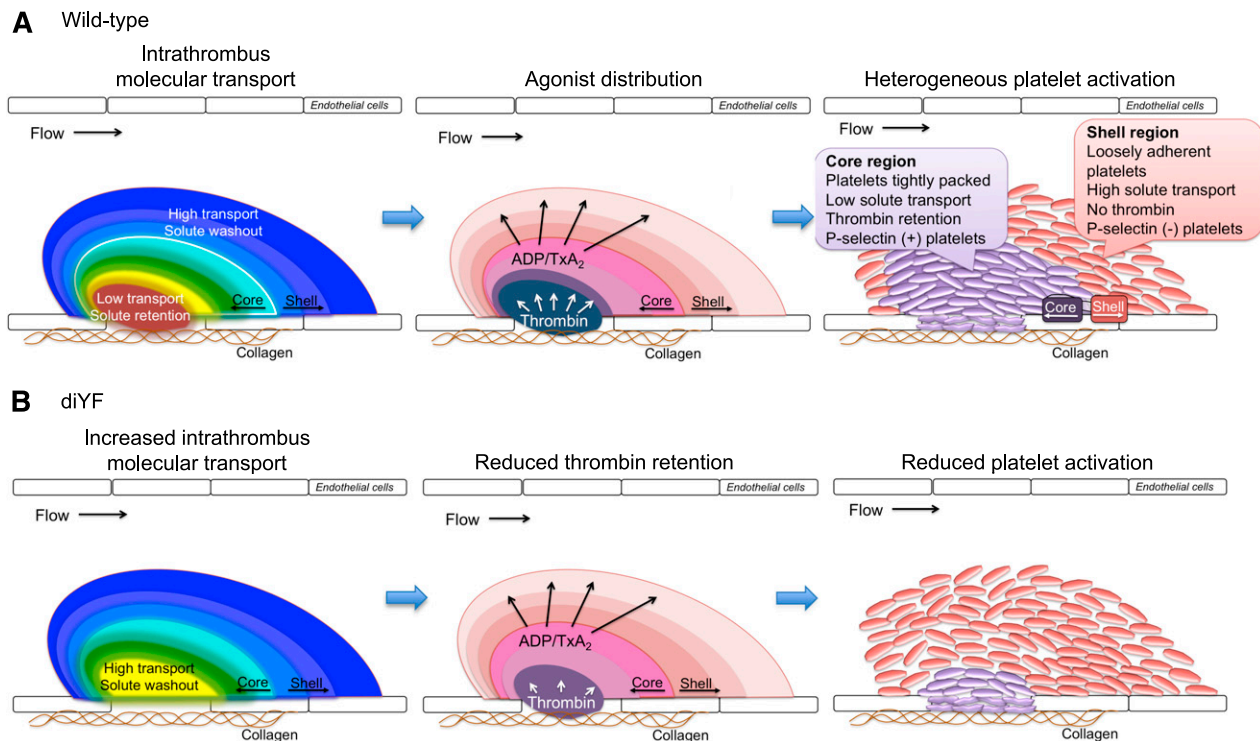


Figure 7. A model for the role of intrathrombus molecular transport in the regulation of agonist distribution and platelet activation. (A) Diagrams show relative gradients of intrathrombus molecular transport rates (left), platelet agonist distribution (middle), and platelet activation (right) following vascular injury in vivo. (B) The impact of impaired $\beta 3$ integrin phosphorylation is shown.

and fibrinolytic enzymes, at a site of vascular injury. In one recent example, Kim et al demonstrated that the density of a fibrin network overlaying a platelet plug has a significant impact on the permeability of solutes moving through the network.²² They found that denser networks reduced permeability such that a larger layer of solute may develop at the boundary between the shell and core regions. This study and others^{23,24} relied on computational models based on thrombus architectures observed using confocal imaging to simulate solute transport. In the first manuscript of this series,⁷ we provide for the first time a description of molecular transport measured directly within a platelet mass in vivo, and relate dynamic changes in intrathrombus molecular transport to changes in platelet mass architecture, thrombin distribution, and platelet activation. The results of that study indicated that irreversible platelet activation is preceded by a decrease in solute transport in the same region of the platelet mass that will become P-selectin positive (ie, the core region). These results are consistent with the finding that porosity of the core region is significantly reduced compared with the shell region with similar kinetics to the platelet mass consolidation observed here. Taken together with the results of studies from the diYF mice, a model emerges in which regulated changes in platelet mass consolidation, dictated at least in part by $\beta 3$ tyrosine phosphorylation–dependent platelet retraction, contribute to an altered hemodynamic microenvironment within the core region of the platelet mass in which molecular transport is slowed and solutes are retained to promote platelet activation (Figure 7).

Several factors determine the movement of molecular species within and/or around a pile of platelets, including the size of the pores (plasma volume) between platelets, how well connected are the pores as well as their spatial distribution, the tortuosity of the pore space, the plasma velocity and the size of the solute. In the second manuscript in this series,⁸ computational modeling studies were performed to examine the importance of each of these variables in determining

molecular transport within a platelet mass, as well as the likely impact of interplatelet molecular transport on the distribution of soluble species generated at a site of injury, such as thrombin. Those studies demonstrate that as platelets accumulate and become tightly packed, molecular movement is primarily determined by the effective diffusion of the molecular species. In other words, the small gaps between platelets within a hemostatic plug or thrombus, particularly in the core region where they are most tightly packed, provide a microenvironment where soluble species are protected from washout. Furthermore, differences in physical factors between the core and shell regions suggest that retention of soluble species within the core region not only has the potential to promote platelet activation in that region, but may also provide a mechanism to limit the extension of hemostatic plug. The data in the present study indicate that platelet mass consolidation is a critical component regulating molecular transport within a platelet plug, as reduced consolidation in diYF mice resulted in increased solute transport during platelet plug formation. They further provide evidence supporting a model in which the consequences of increased solute transport include reduced concentration/distribution of bioactive molecules, as demonstrated by the finding of decreased thrombin activity and decreased platelet activation in diYF thrombi. It should be noted, however, that whereas we have ruled out several possibilities for direct effects of the diYF mutation on platelet activation, we cannot at present rule out the possibility that other, currently unappreciated, effects of the diYF mutation could also contribute.

Although we have not explicitly considered the contribution of fibrin(ogen) to solute transport in this study, it likely plays an important role. Indeed, the contribution of fibrin to solute transport is captured in our in vivo measurements, as fibrin is present within the developing platelet mass. Similarly, the physical properties used to define our computational model included the contribution of fibrin as these were based on our in vivo measurements where fibrin was present.

With regard to solute transport, the expected impact of fibrin formation would be similar to platelet retraction shrinking the spaces between platelets, for example, decreased pore volume and increased tortuosity. In addition, several pro- and anti-coagulant proteins (including thrombin itself) bind to fibrin, further impacting their distribution within a platelet mass. Additional approaches are required to tease out the precise contribution fibrin, but are beyond the scope of the current study.

In conclusion, we have demonstrated a novel role for $\alpha_{IIb}\beta_3$ outside-in signaling in the regulation of platelet mass consolidation in vivo. Furthermore, we provided evidence that the extent of platelet packing in a hemostatic plug regulates interplatelet molecular transport, agonist distribution, and subsequent platelet activation. Taken together, these observations demonstrate that optimal hemostatic plug formation results from the interaction of physics, biochemistry, and cell biology.

Acknowledgments

This work was supported by the American Heart Association (11SDG5720011 [T.J.S.]) and the National Heart, Lung and Blood Institute (P01HL40387 [L.F.B.]; R01HL119070 [T.J.S. and L.F.B.]; and R01HL103419 [S.L.D. and L.F.B.]). J.D.W. and M.T. were

supported by NIH training grant T32-HL07439. T.V.C. was supported by NIH training grant T32-HL07971. The confocal intravital microscopy system used was partially funded by National Institutes of Health–National Center for Research Resources (NIH-NCRR) shared instrument grant 1S10RR26716-1.

Authorship

Contribution: T.J.S. designed and conducted experiments, analyzed data, and wrote the manuscript; J.D.W., M.T., J.W., and T.V.C. conducted experiments, analyzed data, and edited the manuscript; and S.L.D. and L.F.B. analyzed and interpreted data, and edited the manuscript.

Conflict-of-interest disclosure: The authors declare no competing interests.

Correspondence: Timothy J. Stalker, Perelman School of Medicine, University of Pennsylvania, 809 BRB II/III, 421 Curie Blvd, Philadelphia, PA 19104; e-mail: tstalker@mail.med.upenn.edu; and Lawrence F. Brass, Perelman School of Medicine, University of Pennsylvania, 815 BRB II/III, 421 Curie Blvd, Philadelphia, PA 19104; e-mail: brass@mail.med.upenn.edu.

References

- Bellido-Martin L, Chen V, Jasuja R, Furie B, Furie BC. Imaging fibrin formation and platelet and endothelial cell activation in vivo. *Thromb Haemost*. 2011;105(5):776-782.
- Dubois C, Panicot-Dubois L, Gainer JF, Furie BC, Furie B. Thrombin-initiated platelet activation in vivo is vWF independent during thrombus formation in a laser injury model. *J Clin Invest*. 2007;117(4):953-960.
- Gross PL, Furie BC, Merrill-Skoloff G, Chou J, Furie B. Leukocyte-versus microparticle-mediated tissue factor transfer during arteriolar thrombus development. *J Leukoc Biol*. 2005;78(6):1318-1326.
- Hayashi T, Mogami H, Murakami Y, et al. Real-time analysis of platelet aggregation and procoagulant activity during thrombus formation in vivo. *Pflugers Arch*. 2008;456(6):1239-1251.
- Stalker TJ, Traxler EA, Wu J, et al. Hierarchical organization in the hemostatic response and its relationship to the platelet-signaling network. *Blood*. 2013;121(10):1875-1885.
- van Gestel MA, Heemskerck JW, Slaaf DW, et al. Real-time detection of activation patterns in individual platelets during thromboembolism in vivo: differences between thrombus growth and embolus formation. *J Vasc Res*. 2002;39(6):534-543.
- Welsh JD, Stalker TJ, Voronov R, et al. A systems approach to hemostasis: 1. The interdependence of thrombus architecture and agonist movements in the gaps between platelets. *Blood*. 2014;124(11):1808-1815.
- Tomaiuolo M, Stalker TJ, Welsh JD, Diamond SL, Sinno T, Brass LF. A systems approach to hemostasis: 2. Computational analysis of molecular transport in the thrombus microenvironment. *Blood*. 2014;124(11):1816-1823.
- Ono A, Westein E, Hsiao S, et al. Identification of a fibrin-independent platelet contractile mechanism regulating primary hemostasis and thrombus growth. *Blood*. 2008;112(1):90-99.
- Calaminus SD, Auger JM, McCarty OJ, Wakelam MJ, Machesky LM, Watson SP. MyosinIIa contractility is required for maintenance of platelet structure during spreading on collagen and contributes to thrombus stability. *J Thromb Haemost*. 2007;5(10):2136-2145.
- Law DA, DeGuzman FR, Heiser P, Ministri-Madrid K, Killeen N, Phillips DR. Integrin cytoplasmic tyrosine motif is required for outside-in $\alpha_{IIb}\beta_3$ signalling and platelet function. *Nature*. 1999;401(6755):808-811.
- Mahabeleshwar GH, Feng W, Phillips DR, Byzova TV. Integrin signaling is critical for pathological angiogenesis. *J Exp Med*. 2006;203(11):2495-2507.
- Falati S, Gross P, Merrill-Skoloff G, Furie BC, Furie B. Real-time in vivo imaging of platelets, tissue factor and fibrin during arterial thrombus formation in the mouse. *Nat Med*. 2002;8(10):1175-1181.
- Brinkman HC. A calculation of the viscous force exerted by a flowing fluid on a dense swarm of particles. *Appl Sci Res*. 1947;A1:27-34.
- Dubois C, Panicot-Dubois L, Merrill-Skoloff G, Furie B, Furie BC. Glycoprotein VI-dependent and -independent pathways of thrombus formation in vivo. *Blood*. 2006;107(10):3902-3906.
- Vandendries ER, Hamilton JR, Coughlin SR, Furie B, Furie BC. Par4 is required for platelet thrombus propagation but not fibrin generation in a mouse model of thrombosis. *Proc Natl Acad Sci USA*. 2007;104(1):288-292.
- Hathcock JJ, Nemerson Y. Platelet deposition inhibits tissue factor activity: in vitro clots are impermeable to factor Xa. *Blood*. 2004;104(1):123-127.
- Kuharsky AL, Fogelson AL. Surface-mediated control of blood coagulation: the role of binding site densities and platelet deposition. *Biophys J*. 2001;80(3):1050-1074.
- Leiderman K, Fogelson AL. The influence of hindered transport on the development of platelet thrombi under flow. *Bull Math Biol*. 2013;75(8):1255-1283.
- Spero RC, Sircar RK, Schubert R, Taylor RM II, Wolberg AS, Superfine R. Nanoparticle diffusion measures bulk clot permeability. *Biophys J*. 2011;101(4):943-950.
- Wufus AR, Macera NE, Neeves KB. The hydraulic permeability of blood clots as a function of fibrin and platelet density. *Biophys J*. 2013;104(8):1812-1823.
- Kim OV, Xu Z, Rosen ED, Alber MS. Fibrin networks regulate protein transport during thrombus development. *PLoS Comput Biol*. 2013;9(6):e1003095.
- Voronov RS, Stalker TJ, Brass LF, Diamond SL. Simulation of intrathrombus fluid and solute transport using in vivo clot structures with single platelet resolution. *Ann Biomed Eng*. 2013;41(6):1297-1307.
- Xu Z, Lioi J, Mu J, et al. A multiscale model of venous thrombus formation with surface-mediated control of blood coagulation cascade. *Biophys J*. 2010;98(9):1723-1732.